# ON THE DISTRIBUTION OF LATERAL LOADS FOR PUSHOVER ANALYSIS

**P. Colajanni[1] and B. Potenzone[2]**

[1] *AssociateProfessor, Dept. of Civil Engineering , University of Messina, Messina. Italy*
[2] *Assistant Researcher., Dept. of Civil Engineering , University of Messina, Messina. Italy*
*Email: pieroc@ingegneria.unime.it, barbarapotenzone@ingegneria.unime.it*

**ABSTRACT :**

Two new simplified adaptive load patterns for pushover analyses are proposed, able to provide an accurate and on safe side assessment of the actual non linear dynamic response, by enveloping the results provided by using the two load vectors. Initially it will be shown how the input modelling can affect the assessment of the response parameters in Non-Liner Response History Analysis (NRHA), which will be assumed as benchmark to judge the effectiveness of the proposed load patterns. Then, the two new load patterns are presented and their effectiveness in reproducing the results provided by NRHA are compared with those of invariant and adaptive load patterns suggested by seismic codes and proposed in literature, for two structures of different typologies. To this aim, criteria for choosing target displacement in POA are shortly discussed.

**KEYWORDS:** pushover curve, load patterns, non liner static analysis, input modelling, seismic codes.

## 1. INTRODUCTION

Non Linear Static Analysis (NSA) is the most popular method to predict the expected non linear response of the structure under earthquake shaking, and it constitute the analysis tool for upgrades of existing buildings, as well as design of new construction. The main goal in NSA is to directly estimate the plastic deformation demand in ductile elements and the strength demand in members designed to behave elastically.
Building seismic demand assessment by NSA is based upon the pushover or capacity curve, which is evaluated by subjecting a non linear detailed model of the structure to a lateral load pattern of increasing magnitude to generate a total base shear-roof displacement relationship and deformed building configurations. The former is used to evaluate the static and dynamic properties of an equivalent Single-Degree-Of-Freedom (SDOF) oscillator used for assessment of expected global displacement demand, named target displacement, that usually represent the roof displacement of the actual MDOF. The Capacity Spectrum Method (EC8, ATC-40) or the Coefficient Method (FEMA 356) are usually adopted to predict the target displacement, even if a simplified non linear dynamic analysis with the equivalent SDOF can also be performed.
The deformed building configurations are used to relate the local deformation demand and strength demand in elastic and inelastic structural members to the roof displacement, assumed as the global displacement parameter.
The accuracy of NSA is strongly related to three assumptions: i) the load pattern used in performing pushover analyses, that influences both the capacity curve and the distribution of seismic demand along the height of the structure; ii) the procedure to derive the mechanic and dynamic parameters of the equivalent SDOF from the pushover curve;; iii) the estimation of the target displacement.
It has to be emphasized that the actual maximum global displacement for the MDOF system can differ from the equivalent SDOF approximation. Moreover, in NRHA maximum storey drifts and the related maxima of the local deformation parameters are not always attained at the same time among themselves, neither at the same time of the maximum roof displacements. Lastly, the distribution of forces on the structure changes continuously during an earthquake, since the dynamic characteristics of the ground motion itself and the changing into structure stiffness matrix due to member yielding have key influences. Therefore the evolution of force pattern that allow the reproduction by Push-Over Analysis (POA) of the maxima of the response parameters attained during the actual non linear dynamic response is very difficult to assess.

In this context, two new semplificative adaptive load patterns are here proposed, able to provide an accurate and on safe side assessment of the actual non linear dynamic response.
Initially it will be shown how the input modelling can affect the assessment of the response parameters in NRHA, which will be assumed as benchmark to judge the effectiveness of the proposed load patterns.
Then, the two new load patterns are presented and their efficiency in reproducing the results provided by NRHA are compared with those of invariant and adaptive load patterns suggested by seismic codes and proposed in literature, for two structures of different typologies. To this aim, criteria for choosing target displacement in POA are shortly discussed.

## 2. INFLUENCE OF INPUT MODELLING

The efficiency of POA procedures and load vectors for prediction of seismic demand are usually assessed by comparison with the results provided by NRHA. However, during an earthquake, the distribution along the height of the seismic demand is strongly influenced by the characteristic of the seismic excitation, and the results are very scattered. To stress this circumstance, the local seismic response in two structures, excited by two different sets of seismic input are compared.
The first structure is a square plan 12 storey steel building (Colajanni and Potenzone, 2008) made up of four three bay pinned steel frames in each direction, having bay length 8m and storey height 3.2 m. Seismic action is withstood by 4 K eccentrically braced frames only (Figure 1), located in the four central bays of the external frames, with short links having length $e$=0.1 $l_t$, pinned beam to column joints and columns pinned at the base. The structures have been designed to carry dead and live storey loads of $G_k$=4.4 kN/m$^2$ and $Q_k$=2.0 kN/m$^2$ respectively, and seismic design action evaluated according to EC8 for soil type B and peak ground acceleration (PGA) of 0.35g, assuming a behaviour factor $q$=6. In Table 2.1 designed element cross sections are reported. The fundamental period of vibration is 1.78 sec.

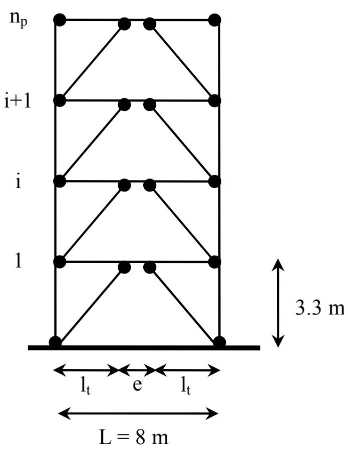


Figure 1 Steel EBFs configurations

Table 2.1 Data for structural sections of steel EBFs

Section steel: FE 360, except sections marked by superscript [1] that have steel FE 430

8 STOREY

| ST. | LINKS | COLOUMNS. | BRACES |
|---|---|---|---|
| 8 | HEA 180 | HEA 180 | HEM 120 |
| 7 | HEB 200 | HEA 180 | HEM 140 |
| 6 | HEB 240 | HEB 240 | HEM 140 |
| 5 | HEB 280 | HEB 240 | HEM 160 |
| 4 | HEB 300 | HEB 320 | HEM 160 |
| 3 | HEB 320 | HEB 320 | HEM 180 |
| 2 | HEB 320 | HEM 320 | HEM 180 |
| 1 | HEB 340 | HEM 320 | HEM 180 |

12 STOREY

| ST. | LINKS | COLOUMNS. | BRACES |
|---|---|---|---|
| 12 | HEA 160 | HEA 180 | HEM 120 |
| 11 | HEB 180 | HEA 180 | HEM 140 |
| 10 | HEB 220 | HEB 240 | HEM 140 |
| 9 | HEB 240 | HEB 240 | HEM 160 |
| 8 | HEB 260 | HEB 300[1] | HEM 160 |
| 7 | HEB 280 | HEB 300[1] | HEM 180 |
| 6 | HEB 300 | HEB 340[1] | HEM 180 |
| 5 | HEB 300 | HEM 3401 | HEM 180 |
| 4 | HEB 320 | HEM 340[1] | HEM 180 |
| 3 | HEB 340 | HEM 340[1] | HEM 180 |
| 2 | HEB 340 | HEM 340[1] | HEM 200 |
| 1 | HEB 340 | HEM 340v | HEM 200 |

The first set of seismic excitation samples is made of seven recorded accelerograms chosen so that mean response spectrum match the Eurocode 8 type B elastic response spectrum for a Peak Ground Acceleration $a_{g,max}$ (PGA) of 0.35g, and available at the web site htpp://www.reluis.it. The second set is made of 30 artificially accelerograms generated so that to be spettro-compatible (Cacciola et al. 2004) with the previous mentioned elastic response spectrum, with strong motion stationary phase of 30 sec. Both the sets of accelerograms are scaled to the PGA value $a_{g,max}$=0.15$g$ that produce the attainment of the link collapse plastic rotation $\gamma_u$=0.09 *rad* at the 12th storey. In Figures 8a, 8b and 8c the non dimensional mean values (solid line) and the maximum values (dashed line) of the maxima of story displacements U/H (H=structure total height), storey drifts $\Delta$U/h (h=storey height), and link plastic rotations $\gamma/\gamma_u$ respectively for the two sets are compared. The figures shown that, while the distributions of the mean values of the three response parameters are almost coincident, the maxima values are strongly different. Remarkably, the maxima of the response parameters for the recorded accelerograms are often more than twice the mean value of the maxima. The large scattered for recorder accelerograms is stressed in Figures 3a, 3b and 3c where the corresponding values of the Coefficient of Variations (COV) are shown. COV values for recorded accelerograms (R) are very large and varies in the range 0.5<COV<0.9 for storey displacements and storey drifts, and in the range 0.65<COV<1.2 for link plastic rotations. The very large scattered of the results are due mainly to the ground motion characteristics, and also to the low redundancy of the structural scheme where only the EBFs withstand the horizontal seismic actions.

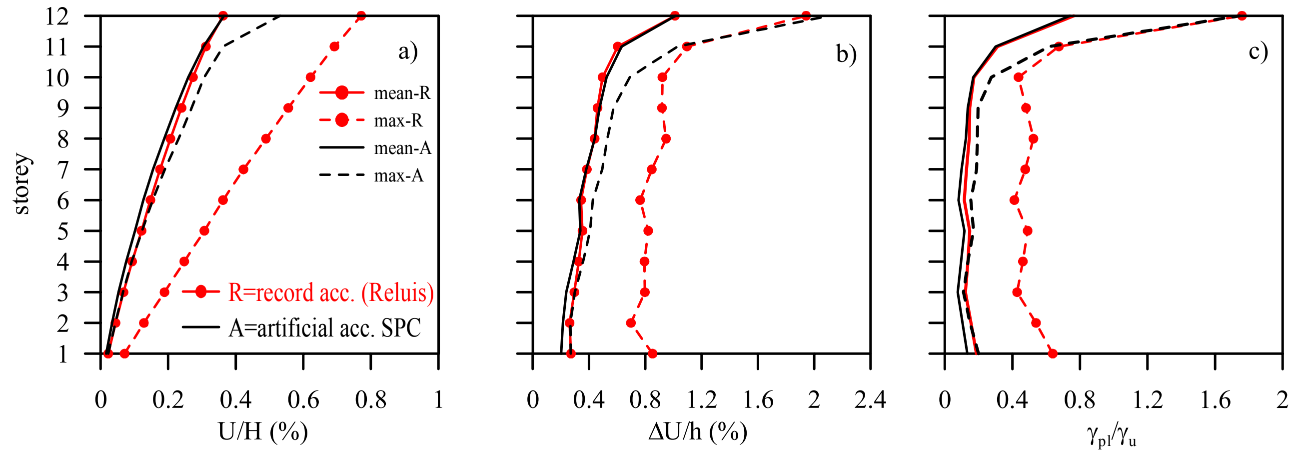


Figure 2: 8 storey EBF response parameters for recorded and artificially generated accelerograms

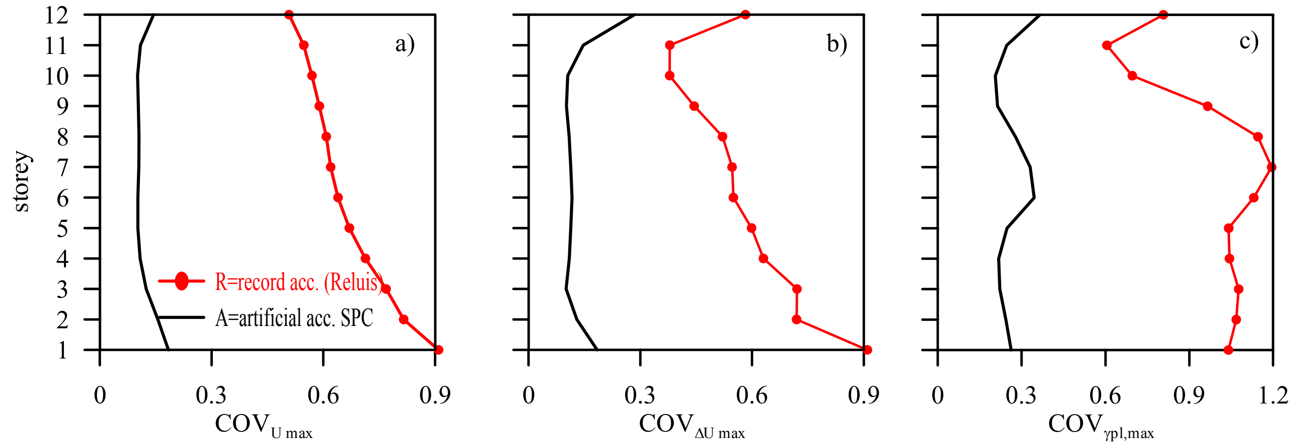


Figure 3: COV of EBF response parameters for recorded and artificially generated accelerograms

The second illustrative example is the six storey irregular concrete Moment Resistant Frame (MRF) depicted in Figure 4a, constructed with steel having yield strength $f_y$=414 MPa and concrete strength $f'_{c0}$=30 MPa, designed to carry dead vertical load of 20 kN/m and a seismic excitation with PGA=0.35 $g$, and has a fundamental period of vibration of $T_1$=0.98 sec. In Figures 4b and 4c the curves of the non dimensional mean values and the maximum values of the maxima of story displacements U/H and storey drifts ΔU/h obtained for the two sets of seismic excitation are compared. For this irregular frame the maximum values of storey displacements are noticeable larger than the mean values, even for artificially generated accelerograms. Moreover, the mean values of storey drifts also are different between the results obtained with the two sets of accelerograms. Lastly, in Figures 5a and 5b the corresponding curves of the COV show that for this more redundant structural typology the results are less scattered than those obtained for the EBF.
The results shown in this section stress that distributions along the height of the response parameters for recorded accelerograms are very scattered. Therefore NSP must be formulated to provide assessment on the safe side of the expected seismic demand for expected seismic excitation, rather than closely reproduce the results pertaining to a single sample of the input. To this aim, appealing and effective appears the procedure suggested by recent seismic codes (EC8, FEMA 356, ATC-40) that require the assessment of the seismic demand by enveloping the results provided by POA performed by using two different load patterns.

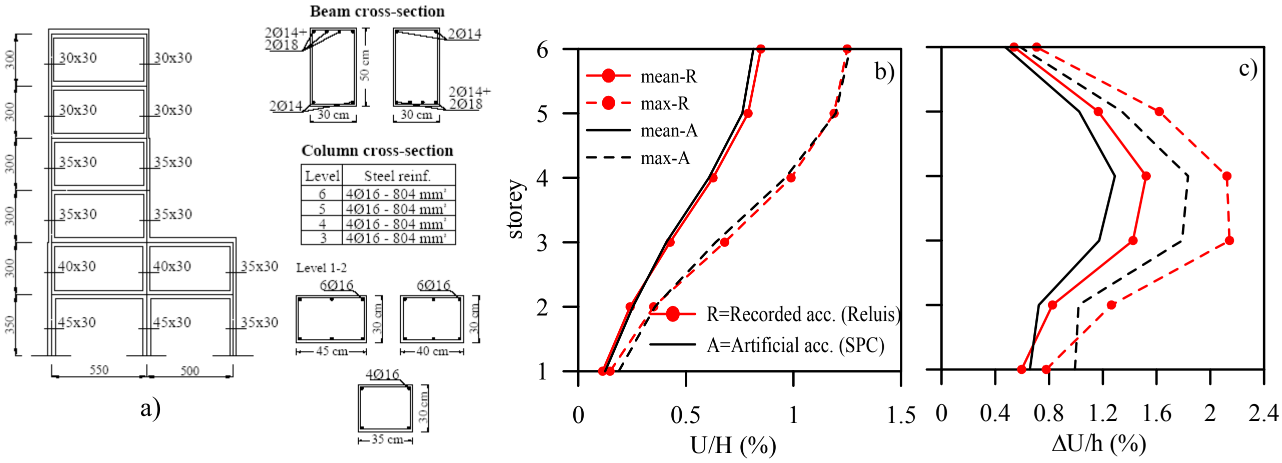


Figure 4. Irregular concrete MRF: a) structural scheme and element cross sections; b and c) mean of the maxima and maxima of response parameters for recorder (R) and artificially generated accelerograms.

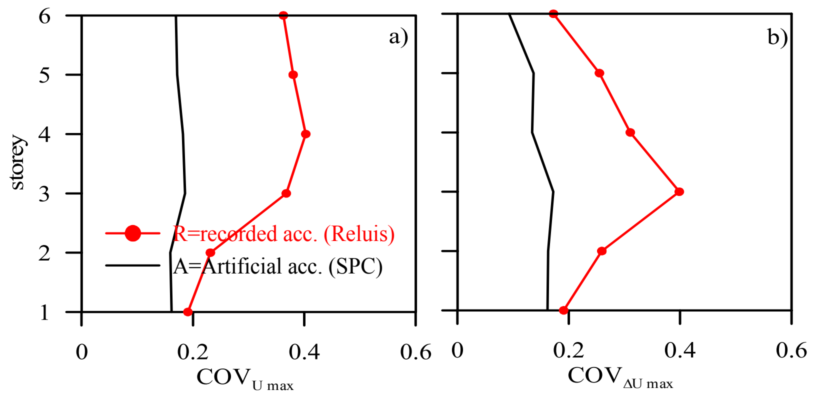


Figure 5 COV of MRF response parameters for recorded and artificially generated accelerograms

## 3. TWO NEW SEMPLIFIED ADAPTIVE LOAD PATTERNS

With the aim of bounding the likely distribution of storey drifts and local ductility demands along the height of the structure, seismic codes require that POA is performed enveloping the results obtained by using two different seismic force patterns pertaining to two groups: - a load pattern aimed at reproducing the distribution of seismic forces acting on the structure in the elastic state, chosen in a first group collecting triangular, first mode and the pattern that reproduce the distribution of storey shear in elastic modal analysis, named SRSS; - a load pattern aimed at bounding or reproducing the change in distribution of seismic forces due to progressive yielding of the structure, chosen in a second group collecting the uniform and adaptive load patterns.
Numerical analysis performed in the last decade have shown that uniform load vector led to notably large errors, especially for lower floors, where excessively large response are predicted, while the use of single or multimodal adaptive load vectors implies unwarranted increment of accuracy.
In this context, two new simplified adaptive load patterns are proposed, obtained as a combination of known load distributions reported in FEMA 440. Their formulation is based on extensive analytical and numerical investigations that have shown that, during an adaptive POA; the SRSS load pattern is the most accurate pattern in providing maximum member forces in the elastic phase. By contrast, a criterion of theoretical derivation to define an effective load distribution, when structural elements overcome the yielding strength, is not yet available. However it is easy to predict by simple consideration on the static response of shear type frames that, once the target displacement at the roof level is fixed to reproduce the actual response of the MDOF structure, by using a uniform load vector the seismic demand at the lower floor is over estimated, while by using the load vector with acceleration proportional to the square of the story height above the foundation level, the response at the upper storeys is over estimated too.

In order to minimize the scattering between the actual and the predicted response, these two simplified distribution are used only in the post-yielding phase. Therefore, the two proposed simplified adaptive load has the same load vector in the elastic phase, coincident with the SRSS load vector :

$$F_i = \alpha_1 \left( V_i - V_{i+1} \right) \qquad i = 1, 2, \ldots n-1; \quad F_n = \alpha_1 V_n \qquad 0 \le \alpha_1 \le \alpha_y \tag{3.1}$$

where $V_i$ is the storey shear provided by a conventional multimodal elastic dynamic analysis, $\alpha_1$ is the load factor, and $\alpha_y$ is its value at the first yielding. After yielding, in the first proposed load vector, named Prop A, the force increments are distributed along the height according to the uniform pattern, as follows:

$$F_i = \alpha_y \left( V_i - V_{i+1} \right) + \alpha_2 W_i \quad i = 1, 2, \ldots n-1; \quad F_n = \alpha_y V_n + \alpha_2 W_2 \qquad 0 \le \alpha_2 \tag{3.2}$$

where $W_i$ is the storey seismic weight, and $\alpha_2$ the new load factor. In the proposed second load vector, named Prop. A2, the force increments after the first yielding are distributed according the FEMA 440 parabolic "code distributions"(P) as follows:

$$F_i = \alpha_y \left( V_i - V_{i+1} \right) + \alpha_2 W_i z_i^2 \quad i = 1, 2, \ldots n-1; \quad F_n = \alpha_y V_n + \alpha_2 W_2 \qquad 0 \le \alpha_2 \tag{3.3}$$

where $z_i$ is the *i-th* storey rise above the foundation level.
To assess the efficiency of the proposed load vectors, in the next sections preliminarily, the results in the estimate of target displacement obtained by several load patterns are compared with the results obtained by NRHA.

## 4. ESTIMATE OF TARGET DISPLACEMENT

One of the key issues in POA is the evaluation of the target displacement, performed on the basis of the dynamic and mechanic parameters of the equivalent SDOF, derived by means of the capacity curve. In Figure 6a and 6b the capacity curves obtained by different load vectors are compared for the 8 storey EBF (see Tab. 2.1) and the six storey concrete MRF: Namely, the load pattern corresponding to storey shears derived by multimodal elastic dynamic analysis (SRSS), the uniform (U) and the multimodal force-based adaptive (FAPM) load vector, and the multimodal displacement based adaptive procedure (DAPM) (Antoniou and Pinho 2004) and the two simplified adaptive load vectors based on SRSS+U (Prop A) and SRSS+P (Prop. A2). In the figure the dynamic curve obtained via the Incremental non-linear Dynamic Analyses (IDA), performed for the 30 samples of the artificially generated input by progressively increasing the PGA, and evaluating the maximum roof displacement reached at the time $T_{MUr}$ and the corresponding value of the maximum base shear in the time range $T_{MUr}$-$T_1/4 \le t \le T_{MUr}$-$T_1/4$ ($T_1$=fundamental vibration period of the structure) for the EBF is also depicted.

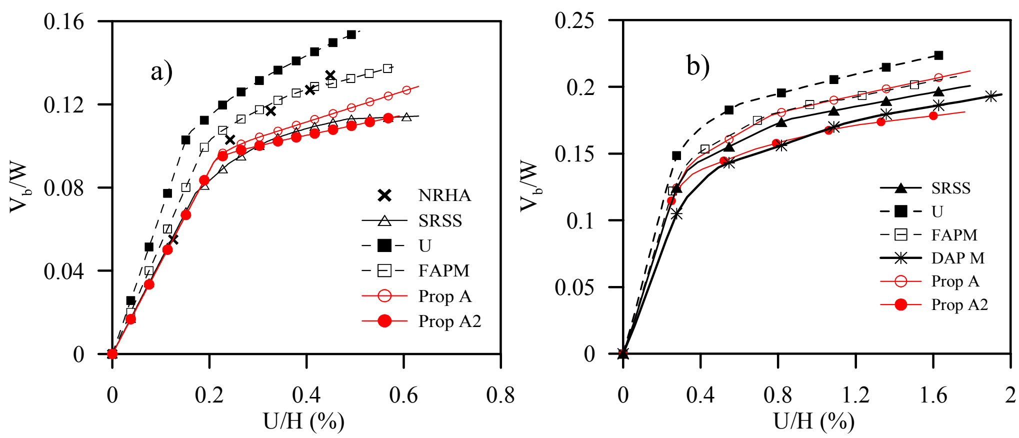


Figure 6 Pushover curves for different load patterns: a) eight story steel EBF; b) six storey concrete MRF

In Table 4.1 the corresponding percentage errors $\varepsilon_U$ (%) in the prediction of the target displacements evaluated by NRHA for the collapse values of PGA, namely $a_{gu}$=0.22g for the EBF and $a_{gu}$=0.60g for the MRF, provided by the Coefficient Method (FEMA 356) for the different load vectors are reported. For both the EBF and the concrete MRF all the load patterns provide a target displacement that is larger than the actual one. Uniform distribution leads to the smaller over-estimation. Let us stress that, in NRHA, the maxima storey drifts at the different levels do not occur at the same instant. In Table 4.2 the two different response parameters obtained by NRHA, namely the maximum roof displacement $U_{rf}$ and the sum of maxima storey drifts $\Sigma\Delta U$ for the two example frames are compared. In both cases $\Sigma\Delta U$ is about 17% larger than $U_{rf}$. Therefore, in order to obtain a prediction of storey drifts and related local deformation demand by POA resembling the NRHA ones, the target displacements should approximate the sum of maximum storey drifts rather than the roof displacement. Thus, most of the predictions of target displacement in Table 4.1 appear to be too much on the safe side, with exception for the uniform load vector.

Table 4.1 Error in assessment of target displacement by POA

| | Steel EBF $a_{gu}$=0.22g -$U_{NRHA}$ =0.119 m | | | | | Concrete MRF $a_{gu}$=0.60g -$U_{NRHA}$ =0.27 m | | | | |
|---|---|---|---|---|---|---|---|---|---|---|
| | 1st gr. | 2nd gr. | | proposed | | 1st gr. | 2nd gr. | | proposed | |
| Load pattern | SRSS | Unif. | FAPM | PropA | PropA2 | SRSS | Unif. | FAPM | PropA | PropA2 |
| $\varepsilon_U$ (%) | 38.65 | 13.44 | 28.57 | 40.33 | 40.33 | 24.25 | 12.85 | 21.3 | 24.4 | 24.4 |

Table 4.2 NRHA results

| | 8 storeys EBF | 6 storeys MRF |
|---|---|---|
| | $a_{gu}$=0.22g | $a_{gu}$=0.60g |
| $U_{rf}$ | 0.118 | 0.264 |
| $\Sigma\Delta U$ | 0.127 | 0.310 |
| $\Sigma\Delta U \backslash U_r$ | 1.185 | 1.172 |

## 5. ASSESEMENT OF RESPONSE PARAMETER DISTRIBUTION ALONG THE HEIGHT.

The efficiency of the different load patterns in reproducing the seismic demand evaluated by NRHA is investigated for the two frames before analysed for the collapse values of PGA. The results obtained by the Modal Pushover Analysis (MPA) proposed by Chopra and Goel (2002) are also reported. Mean values of maximum response parameters for 30 samples of artificial accelerograms are compared with the results of POA, performed by imposing a top storey displacement equal to the mean value $\Sigma\Delta U$ of the sum of storey drifts recorded in NRHA (see Table 4.2). Thus, the distribution of response parameters along the structure height can be checked.
In Figure 7a the storey drift for the EBF are compared, while in Figure 7b the corresponding curves of the percentage errors $s_i$ in estimation of NRHA results by POA are depicted. The curves shown that the SRSS distribution and the MPA procedure are able to reproduce the pattern of storey drift distribution, even if at the intermediate storeys the former and at the first storey the latter provide assessment on unsafe side. In the lower storeys uniform and FAPM distributions predict a storey drift much larger than the dynamic one. By contrast, the Prop.A pattern is the only one among the others patterns that provide a prediction on the safe side at the lower storeys, greatly reducing the errors of uniform and FAPM patterns. Moreover, for this structure the Prop A pattern is effective in providing a prediction of storey drift on the safe side up to the third storey. At the same time, Prob. A2 pattern predicts an accurate and conservative assessment of the response above the third storey, with exception of roof storey where only SRSS is effective. Therefore an accurate and conservative prediction of the response can be obtained by enveloping the results provided by Prop. A and Prop. A2 load vectors. The same consideration can be extended to the results in Figures 8a and 8b, where the curves for the link plastic distortions are depicted.
In Figures 9a and 9b the curves of the storey drifts and percentage errors in its assessment by POA are depicted for the concrete six storey frame. In this case the SRSS and the Prop A2 load patterns, and the DAPM procedure (Antoniou and Pinho, 2004) are the more accurate, even if the former predict underestimation of the response at the upper storeys, while Prop. A2 and DAPM at the lower storeys. By contrast, the Prop. A pattern provides results on the safe side at the lower storeys that are more accurate than those provided by uniform and FAPM distributions, proposed by seismic code as the distribution of the second group. Once more an accurate and on the safe side prediction of the storey drifts along all the height of the structure can be obtained by enveloping the results provided by the two proposed distributions. The curves of the largest plastic hinge rotations at each level shown in Figure 9c confirm the above considerations.

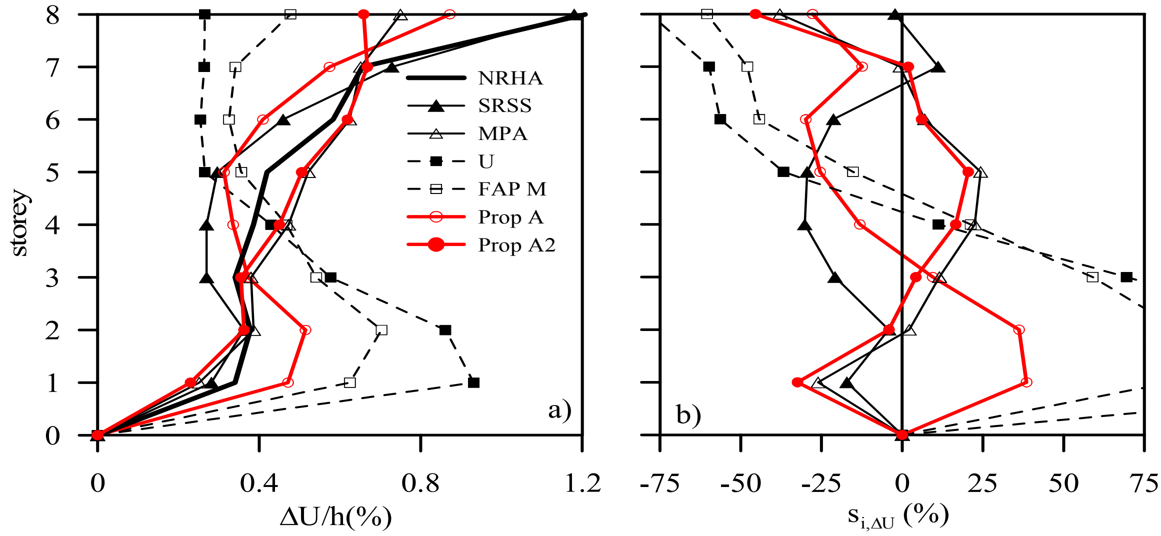


Figure 7: EBF story drifts: a) NRHA and POA patterns; b) percentage errors in prediction by POA

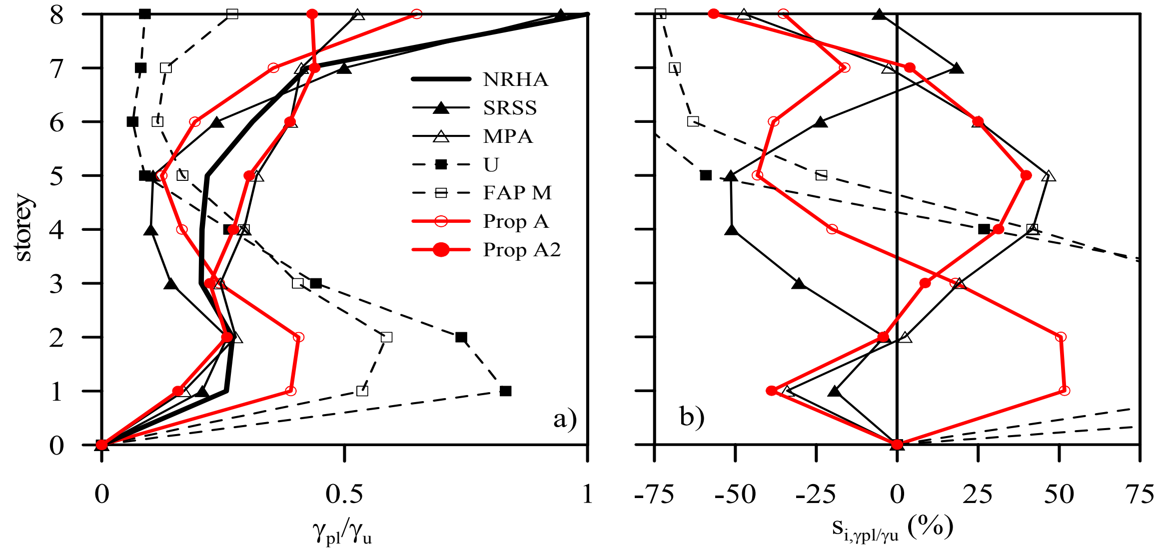


Figure 8 EBF link plastic distortion: a) NRHA and POA patterns; b) percentage errors in prediction by POA

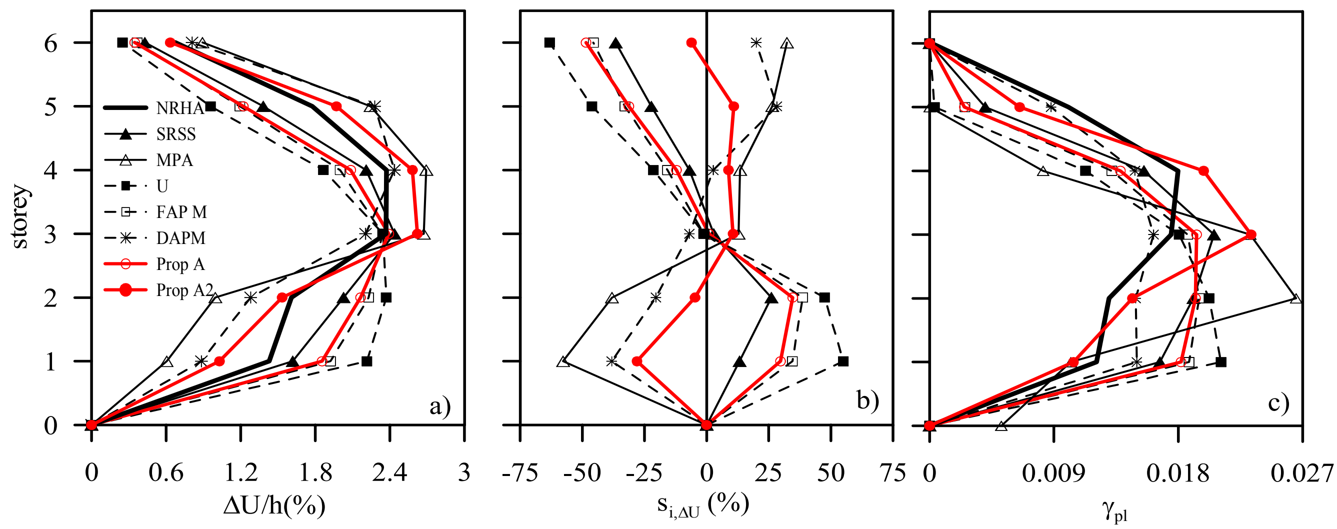


Figure 9 MRF response: a) storey drifts: b) percentage errors in storey drift prediction by POA; c) plastic rotations

Table 5.1 Percentage errors in prediction of NRHA local response parameters provided by POA result envelops

| | Plastic link distortion in the steel EBF | | | | | | Storey drifts in the concrete MRF | | | | | | |
|---|---|---|---|---|---|---|---|---|---|---|---|---|---|
| | seismic codes | | proposed | | | | seismic codes | | | proposed | | | |
| storey. | SRSS+ U | SRSS+ FAP M | SRSS+ propA2 | SRSS+ prop.A | MPA+ prop.A | prop.A+ prop.A2 | SRSS+ U | SRSS+ FAP M | SRSS+ DAPM | SRSS+ Prop.A2 | SRSS+ prop.A | MPA+ prop.A | prop.A+ prop.A2 |
| 1 | 223.98 | 109.06 | **-19.30** | 51.68 | 51.68 | 51.68 | 55.02 | 34.51 | 13.28 | 13.28 | 29.75 | 29.75 | 29.75 |
| 2 | 174.89 | 117.73 | **-3.99** | 50.54 | 50.54 | 50.54 | 47.48 | 38.63 | 26.11 | 26.11 | 34.64 | 34.64 | 34.64 |
| 3 | 115.20 | 96.94 | 8.63 | 17.95 | 19.21 | 17.95 | 2.91 | 2.91 | 2.91 | 10.65 | 2.91 | 12.89 | 10.65 |
| 4 | 26.86 | 41.69 | 31.27 | **-20.10** | 41.82 | 31.27 | **-6.88** | **-6.88** | 2.68 | 8.82 | **-6.88** | 13.50 | 8.82 |
| 5 | **-51.38** | **-23.40** | 39.82 | **-43.16** | 46.80 | 39.82 | **-22.21** | **-22.21** | 28.28 | 10.93 | **-22.21** | 26.37 | 10.93 |
| 6 | **-23.69** | **-23.69** | 24.95 | **-23.69** | 25.26 | 24.95 | **-36.51** | **-36.51** | 19.99 | **-6.06** | **-36.51** | 32.34 | **-6.06** |
| 7 | 18.32 | 18.32 | 18.32 | 18.32 | **-2.62** | 3.89 | | | | | | | |
| 8 | **-5.50** | **-5.50** | **-5.50** | **-5.50** | **-35.16** | **-35.16** | | | | | | | |
| δ | 79.98 | 54.54 | 18.97 | 28.87 | 34.14 | 31.91 | 28.50 | 23.61 | 15.54 | 12.64 | 22.15 | 24.91 | 16.81 |

Lastly, in Table 5.1 the percentage errors in prediction of the plastic rotations in the links for the EBF and the storey drifts for the MRF, obtained according to seismic codes EC8 and FEMA 356, by enveloping the results provided by load patterns of first and second group are compared with those obtained by using the proposed load patterns. In the Table the bold digit stresses the predictions on the unsafe side, while in the last row the average values along the structure height of the absolute values of the errors δ are shown. It can be easily recognized that the envelope of the results provided by the two proposed load patterns can constitute an appealing simple alternative to the distribution suggested by the seismic codes

## 6. CONCLUSIONS

Two new simplified adaptive load patterns for pushover analyses are proposed, able to provide an accurate and on the safe side assessment of the actual non linear dynamic response, by enveloping the results provided by using the two load vectors.

The analysis of the scattering of the local deformation demand obtained by NRHA performed with recorded samples of seismic excitation lead to conclude that a reasonable approach in Non Linear Static Analysis have to aims at bounding the expected seismic response by enveloping the results provided by POA performed by using two different load patterns. Numerical analyses have shown that in order to obtain a prediction of storey drifts and related local deformation demand by POA resembling the NRHA ones, the target displacements should approximate the sum of maximum storey drifts rather than the roof displacement. Lastly, favourable comparison of the efficiency of proposed load patterns against those suggested by seismic codes have shown that they can constitute an appealing simple alternative to the load distribution suggested by the seismic codes

## REFERENCES

Antoniou S., and Pinho R. (2004): Development and verification of a displacement-based adaptive pushover procedure, *Journal of Earthquake Engineering*, **8:5**, 643-661 Imperial College Press

Cacciola P., Colajanni P. and Muscolino G. (2004). Combination of modal responses consistent with seismic input representation, Journal of Structural Engineering, ASCE , **130:1**, pp: 47-55.

Colajanni P. and Potenzone, B. (2008). Influence Of Lateral Load Distributions On Pushover Analysis Effectiveness, American Istitute of Phisics, AIP Conference Proceedings, **1020,** Mercea Conf., Rggio Calabria, Italy, pp 880-887.

Chopra A. K. and Goel R.K. (2002). A modal pushover analysis procedure for estimating seismic demands for buildings", *Earthquake Engineering and Structural Dynamics*, **31**, pp: 561-582.

Fema 440 (2005): "Evaluation and improvement of inelastic seismic analysis procedure", Federal Emergency Management Agency, Washington (USA).